

## Adsorption of cesium on polyaniline montmorillonite nanotube-based composite from aqueous solution

R. Saberi<sup>a,\*</sup>, A. Nilchi<sup>b</sup>, E. Mohammad Ghasemi<sup>c</sup>, A.T. Ardeshir<sup>d</sup>, A. Mozaffari<sup>e</sup>

<sup>a</sup>Nuclear Science and Technology Research Institute (NSTRI), P.O. Box: 11365-8486, Tehran, Iran, Tel. +98 2188221128; email: rsaberi@aeoi.org.ir

<sup>b</sup>Materials and Nuclear Research School, Nuclear Science and Technology Research Institute (NSTRI), Tehran, Iran, email: anilchi@gmail.com

<sup>c</sup>Natural Resources Department, Islamic Azad University of Damavand, Tehran, Iran, email: E.M.Ghasemi@outlook.com

<sup>d</sup>Iran Nuclear Regulatory Authority (INRA), P.O. Box: 11365-8486, Tehran, Iran, email: aardeshir@aeoi.org.ir

<sup>e</sup>Civil engineering Department, Politecnico di Milano, Milan, Italy, email: ali.mozaffari@mail.polimi.it

Received 22 October 2018; Accepted 9 June 2019

---

### ABSTRACT

Synthesis of polyaniline-montmorillonite nanocomposite (PANI/MMT) was carried out using a sol-gel method to investigate its cesium adsorption ability. Synthesized PANI/MMT nanocomposite was characterized by using the X-ray diffraction analysis, infrared spectroscopy, scanning electron microscopy and transmission electron microscopy in the laboratory. The effect of different parameters such as pH, contact time, temperature and concentration on the adsorption process was studied and the optimum conditions were obtained. Thermodynamics of the process including the Gibbs free energy, enthalpy change and entropy change were also evaluated. The Langmuir and Freundlich isotherm models were also used to describe the equilibrium data. The results indicated that the Langmuir isotherm model best predicts the cesium adsorption on the adsorbent. In addition adsorption thermodynamic parameters were determined and it was observed that the sorption of cesium on the sorbent is an endothermic and spontaneous process. The result indicated that the adsorption initially commences very fast and the maximum adsorption was attained within 120 min, at pH = 8 and at the temperature of 55°C. The results showed that the synthesized nanocomposite was very efficient in cesium cation adsorption from nuclear waste. The effect of ambient temperature showed that the solution containing 50 mg/L cesium was treated at the optimum temperature with a 96% efficiency.

*Keywords:* Waste treatment; Cesium adsorption; Ion exchange; Nanocomposite; Bentonite

---

### 1. Introduction

Surface water and underground water pollution have been one of the most important concerns in recent years. Some kinds of pollutants include radioactive materials, heavy metals, organic and non-organic compounds [1].

One of the most important issues in industrialized countries is to achieve executive solutions for reducing pollution, replacing hazardous materials with nature-friendly materials

and eliminating hazardous materials with the least damage and minimum costs.

One of the important categories of pollutants that are considered to be a serious threat to the environment and harmful for human health are radioactive substances which could be produced and increased by the use of nuclear reactors incidents, radioactive substances in agriculture, industry and medicine. Strontium, cesium, uranium and carbon are famous examples of these radioactive materials.

---

\* Corresponding author.

So far, various types of adsorbents such as natural, synthetic, organic and inorganic adsorbents have been used to remove radionuclides from aqueous solutions such as coal, bentonite, zeolite, kaolinite, manganese oxide, biomass and activated carbon.

Zeolite is used as an inorganic ion exchange material for the separation of cesium and strontium from aqueous solution in a batch and fixed bed process [2].

Recently, several approaches have been developed to make less expensive and more effective adsorbents for adsorbing these materials. For example, the use of nano-scale adsorbent is one of these approaches applied in recent studies [3–6].

In a research conducted by Yang's et al. [7], titanate nanotubes and titanate nanofibers were used for the separation of cesium ions from aqueous solution. Adsorption capability up to 80% for titanate nanotubes was reported at concentrations higher than 250 ppm and full adsorption at concentrations lower than 80 ppm.

Composite adsorbents are used as another approach that is recently considered by researchers. Separation of cobalt, strontium and cesium from radioactive waste was performed using polyacrylonitrile ammonium molybdophosphate. The results showed that this adsorbent had high selectivity for cesium ion [8].

A two-stage method was proposed for the preparation of composite adsorbent porous foam from titanium hexacyanate and silica potassium by Liu et al. [9]. In the first step, amorphous titania was bonded to the porous wall of the Siliciclastic bundles, and then titanium inside the cavity was converted into potassium titanium hexa-acetate. Composite adsorbent showed high adsorption of cesium [9].

The ability of cesium adsorption in carbon monoxide/hexa-acetate/silica cobalt adsorbent as an inorganic adsorbent has been investigated in recent years. Selectivity and separation of cesium ions in the presence of sodium, hydrogen and potassium ions from aqueous solutions were investigated by this adsorbent. The results indicated high adsorption of cesium and selectivity power over this adsorbent [10–16].

Ding and Kanatzidis [17] reported cesium adsorption by a sulfide-based compounding through ionic exchange mechanism in aqueous solution.

Ferrocyanide composite adsorbent prepared from Ni-PdFs on mineral deposits, including calc, bentonite and silica, for the separation of cesium from aqueous solution, is another example of composite adsorbent used for this purpose [18].

It should be noted that some of these approaches are faced with main problems such as high operational costs or the inability to isolate radionuclides completely [19].

Carbon materials are kind of engineering adsorbents that have been widely used to adsorb metals from aqueous solutions. Carbon nanotubes are a new category of this type which was shown to have a very high potential for adsorbing metals from aqueous solutions [20–22].

Due to the porous structure, high surface area, very low mass density, high strength against radiation and high interactions between carbon nanotubes and contaminating molecules, this material is widely used to separate contaminants such as small molecules, organic materials, heavy metals and radionuclides in aqueous solutions [23,24].

Tofighy et al. [25] in order to remove two-capacity heavy metals from aqueous solutions used the plates with deposited carbon nanotubes over it.

In 2005 Vejsada et al. [26] investigated the adsorption of cesium by clay adsorbent. Different types of clay were used for this purpose. The results showed a very high effect of illite, kaolinite and bentonite clay on the adsorption of cesium ion. Also, the reduction of adsorption rate during the treatment process was observed for all clay species. Besides, the comparison of the cesium adsorption rate by bentonite, illite and kaolinite in the same conditions indicates better adsorption of bentonite clay adsorbent. The main reason for this phenomenon is the difference in the ionic exchange mechanism of the used adsorbents [26].

The separation of cobalt, strontium and cesium ions from radioactive wastewater by silicotitanate nanocrystal adsorbent in a batch system was investigated in this study. Adsorption equilibrium analysis was evaluated by the Langmuir isotherm model in different pH values. The results indicated the high selectivity of this adsorbent in the separation of cesium ions from aqueous solution [27].

In another study, Galambos et al. [28] evaluated the effect of gamma radiation on cesium adsorption rate by bentonite. The results of this study showed that the adsorption capacity of bentonite was increased by exposure of gamma rays [28].

Ararem et al. [29] examined the adsorption of cesium from aqueous solution by a mixture of iron oxide and montmorillonite. In this study, the cesium removal efficiency was investigated in different temperatures. The results indicated that the process was exothermic and adsorption rate increased with decreasing the temperature [29].

Based on Ararem et al.'s [29] research on the pH effect on the cesium removal efficiency of an aqueous solution by a binary mixture of iron oxide and montmorillonite, the best pH was reported in the range of 5 and 9. In addition Fan et al. [30] used chitosan coated montmorillonite to remove chromium from aqueous solution and the results indicated that the pseudo-second-order equation model presented the best correlation with the experimental result.

In 2003, Khan [31] studied the effect of pH on the adsorption of cesium, strontium and cobalt ions from aqueous solution by bentonite. The results indicated that increasing cesium ion uptake was subsequent from increasing pH in aqueous solution [31].

## 2. Experimental

### 2.1. Reagents and apparatus

All the chemicals used in this study – montmorillonite (MMT, Czech Republic), aniline hydrochloride (99% pure, Sigma-Aldrich, Germany), ammonium persulfate (99% pure, Sigma-Aldrich, Germany), hydrochloric acid (99% pure, Sigma-Aldrich, Germany), sodium hydroxide (99% pure, BDH Belgium), sulfuric acid solution (98% pure, Sigma-Aldrich, Germany), distilled water (Merck, Germany), silver nitrate (Sigma-Aldrich, Germany) – were of analytical grade and used without further purification.

The chemical analyses and XRD patterns of the MMT and PANI/MMT were obtained by using a PW 1130/90

X-ray diffractometer (Philips, Holland), with Ni-filtered  $K\alpha$  Cu-radiation beam.

The infrared spectra were recorded using a Vector 22 (Bruker) infrared spectrophotometer (Bruker, Germany). The amount of  $\text{Na}^+$ ,  $\text{K}^+$ ,  $\text{Ca}^{2+}$  and  $\text{Mg}^{2+}$  cations was measured by a PerkinElmer atomic absorption spectrometer (AAS) model 843.

The morphological behavior and texture study was carried out using an S360 scanning electron microscope (Oxford) to get SEM images.

Transmission electron microscopy (TEM) measurements were carried out on a 912-AB TEM (Leo Electron) with an accelerating voltage 200 kV by GATAN digital photography system. A Metrohm pH meter model 744 was used for measurement of pH.

## 2.2. Synthesis of PANI/MMT composites

Polyaniline montmorillonite (PANI/MMT) clay composites were synthesized according to the following method, described in the literature [32,33].

5 g dry MMT was dispersed in 100  $\text{cm}^3$  (1  $\text{M}/\text{dm}^3$ ) HCl in 500 mL round bottom flask. 100  $\text{cm}^3$  aniline hydrochloride (1  $\text{M}/\text{dm}^3$ ) was added to MMT dispersion and stirred for 24 h at room temperature.

Afterward, the modified MMT clay was centrifuged and washed several times with distilled water.  $\text{AgNO}_3$  was used for testing of chloride ion existence in mixtures. The gel-like liquid was dried in an oven at 120°C for 2 h. After complete adsorption and intercalation of anilinium monomers (if any) inside clay galleries, ammonium persulfate 0.4 M was added as an oxidant to the mixture to initiate polymerization. The mixture was stirred for 24 h at room temperature. This resulted in the formation of greenish blue emeraldine salt polymeric composite (EMS) which implied doped form of composite (EMS-MMT). After filtration and subsequent washing with distilled water, the PANI/MMT was dried in room temperature for 3–4 d. The polyaniline (PANI) was prepared by a similar procedure without adding MMT.

## 2.3. Adsorption procedure

Batch technique was used for studying adsorption procedure. 0.1 g of the prepared composite and 25 mL of cesium solution (50 mg/L) of the desired pH were shaken with uniform speed 110 rpm for 90 min. The pH values of the solution were adjusted by NaOH and HCl and monitored with a pH meter. All experiments were carried out at 25°C except for the temperatures dependence studies.

## 3. Results and discussion

### 3.1. Adsorbent characterization

#### 3.1.1. X-ray powder diffraction

Fig. 1 shows X-ray powder diffraction patterns of PANI/MMT and raw MMT.

The peak levels in MMT pattern decreased rapidly after aniline polymerization. It shows the homogeneous distribution of polyaniline in the montmorillonite, shorten the layers

and keep strongly the basic clay structure after composite formation.

Small angle X-ray diffraction in Fig. 1 reveals changes in the  $d$  (001) spacing of MMT. Raw MMT illustrated  $d$  (001) spacing at  $2\theta = 6.8^\circ$ , which is corresponding to  $d$  (001) spacing of 6 Å, after polymerization. It means that the distance between silica layers is 6 Å. This is typical for MMT.

Actually, the shape of the peak became near to flat after polymerization. The peak also moved to the lower angle, obviously.

This figure emphasis that probably some materials entered into the MMT galleries by means of an ion exchanger or adsorption mechanisms which consequently resulted in the tiny interlayer spacing deterioration [33].

#### 3.1.2. FTIR

Fig. 2 shows the FTIR spectra of raw MMT and synthesized PANI-MMT composite. The figures showed peaks at 1,450  $\text{cm}^{-1}$  (benzenoid rings) and 1,580  $\text{cm}^{-1}$  (quinoid rings), which are the characteristic peaks of polyaniline. The relative

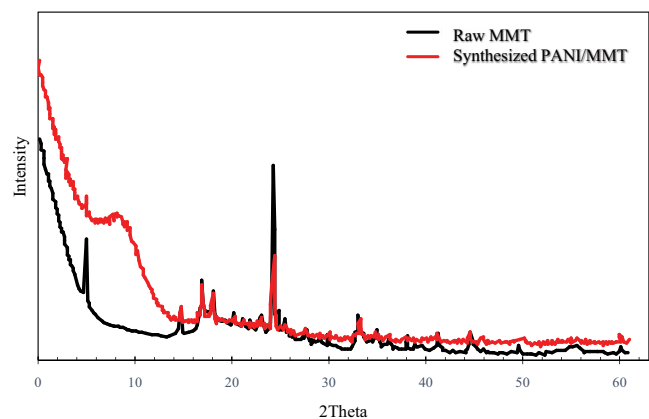


Fig. 1. XRD pattern of MMT and synthesized PANI/MMT sorbent.

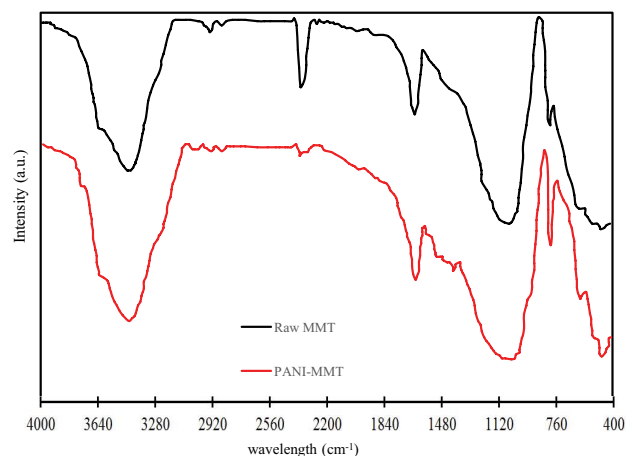


Fig. 2. FTIR spectra of raw MMT and synthesized PANI-MMT nanocomposite.

intensity of the 1,406 and 1,559  $\text{cm}^{-1}$  indicates the oxidation state of the material. For PANI, the peak area ratio was 1.0 the polymer is in the emeraldine salt.

The peaks observed at 463, 518 and 1,057  $\text{cm}^{-1}$  are due to the presence of clay in the composite. Due to the masking effect of polyaniline on clay, it is difficult to detect the presence of polyaniline and clay in this system by using the IR spectrum [31].

### 3.1.3. SEM and TEM

Fig. 3 shows SEM micrograph images of PANI-clay composites. Scanning electron micrograph (SEM) revealed some interesting morphological differences between the pure bentonite clay and PANI-clay composites. The surface of pure clay was flaky texture reflecting its layered structure as shown in Fig. 3. The micrographs of PANI/MMT composite exhibit more ordered and dense structure (smaller sizes with a high density of granules per unit area) comparing with pure clay. It shows that the increase in clay percentage in the preparation solution will increase the compactness. Fig. 4 shows the images of TEM of PANI/MMT produced composite. These figures show that the surface of montmorillonite covered homogeneously by polyaniline. The dimension of the nanoparticles recorded around 100 nm.

## 3.2. Adsorption procedure

### 3.2.1. pH effects

In order to determine the optimum pH at which cesium is effectively adsorbed on PANI/MMT, Cs adsorption was investigated at various pH values (from 2.0 to 10.0). It is observed from Fig. 5 that Cs removal efficiency increase continuously with increasing pH value from 2 (81%) to 8 (93%). This behavior can be attributed to competition between  $\text{H}^+$  and  $\text{Cs}^+$  for adsorption on the PANI/MMT. The maximum sorption was achieved at pH 8.0 (93%).

The Cs removal efficiency decreases sharply with increasing pH from 8 (93%) to 9 (86%). This is due to lower competition between  $\text{H}^+$  and  $\text{Cs}^+$  for adsorption on the PANI/MMT.

### 3.2.2. Effect of contact time

The effect of contact time between cesium solution and PANI/MMT on Cs distribution coefficient was investigated (Fig. 6) for time intervals (10, 20, 30, 60, 120, 180 min). It is obvious that the adsorption percentage increased with increasing the contact time and achieved equilibration in 120 min, then it is maintained constant with increasing the interaction time.

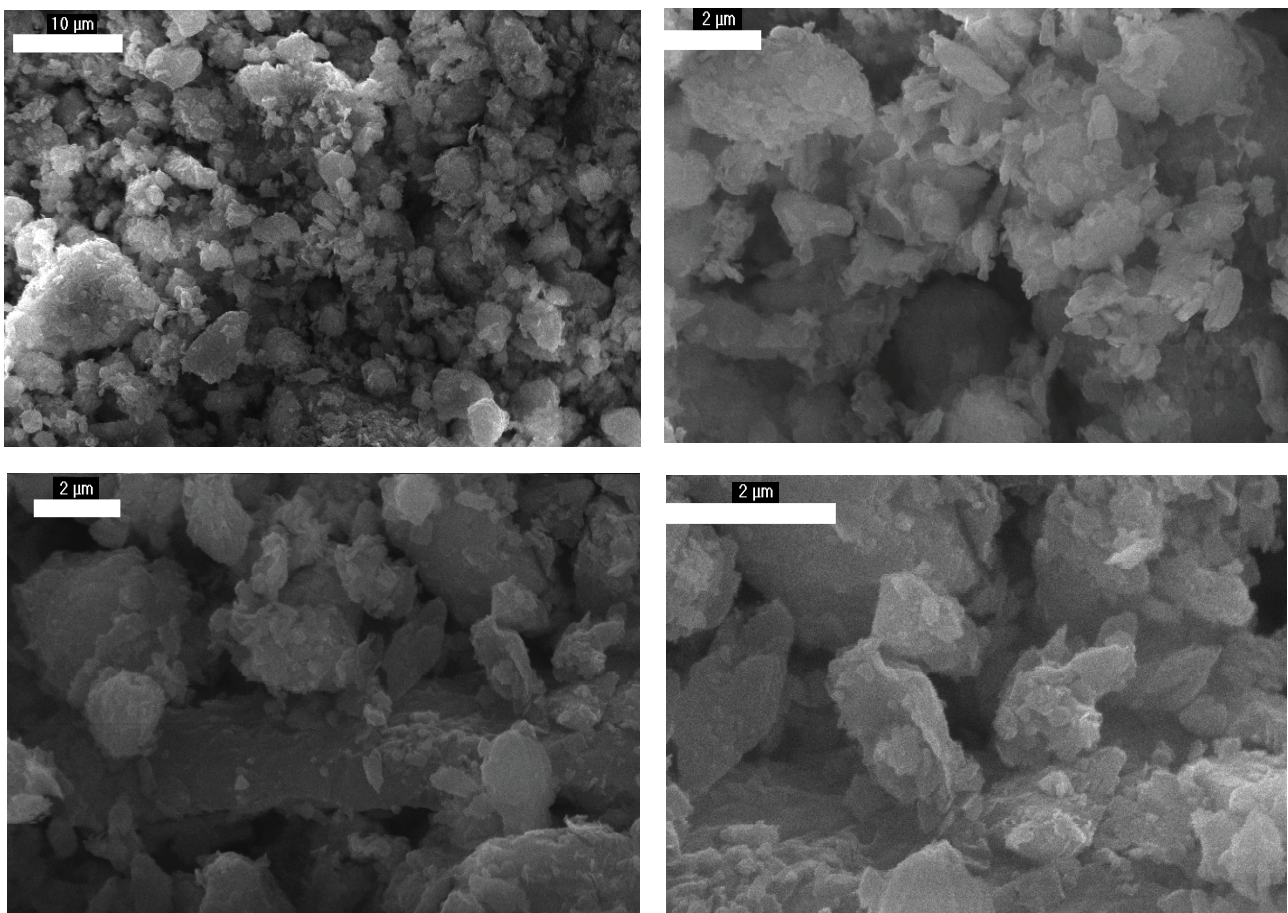


Fig. 3. SEM images of synthesized PANI-MMT.

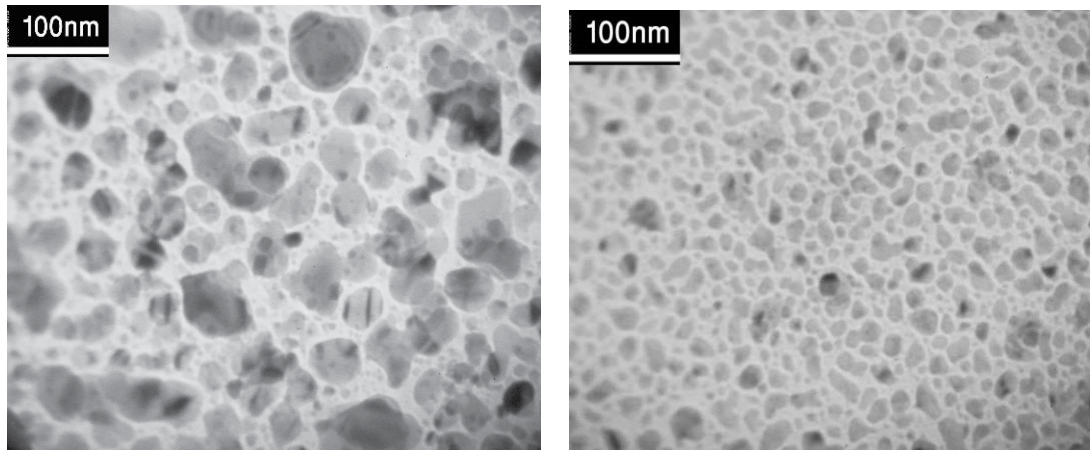


Fig. 4. TEM images of synthesized PANI-MMT.

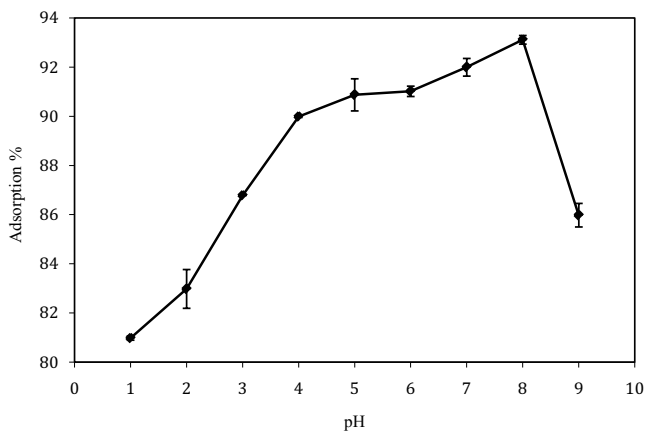


Fig. 5. pH effect on Cs removal.

### 3.2.3. Effect of interfering ions

The effect of  $K^+$ ,  $Na^+$ ,  $Mg^{2+}$  and  $Ca^{2+}$  cations on  $K_d$  of cesium cation was investigated with concentration of  $10^{-4}$  mol/L added in the form of their nitrates to the solution at 298 K. Table 1 indicates that the existence of these cations have significant influence on the adsorption of  $Cs^+$  by PANI/MMT and this effect continuously increases with enhancement of concentration of these interfering cations in the aqueous solution. The effect of  $K^+$  and  $Na^+$  is due to the fact that these cations are from the same group in the periodic table. Furthermore, the interfering effect of  $Mg^{2+}$  and  $Ca^{2+}$  could be due to nonspecific surface adsorption [34].

### 3.2.4. Temperature effect

The effect of temperature on sorption of  $Cs^+$  from aqueous solution using PANI/MMT was investigated from 15°C to 65°C in steps of 10°C while other parameters were kept constant (contact time = 120 min, pH = 8 and  $Cs^+$  concentration = 50 ppm). Fig. 7 shows that the adsorption percentage increased with increasing the temperature from 15°C to 55°C. At this temperature (55°C), complexes were configured but the structure of these complexes is deteriorated with increasing the temperature to more than 55°C.

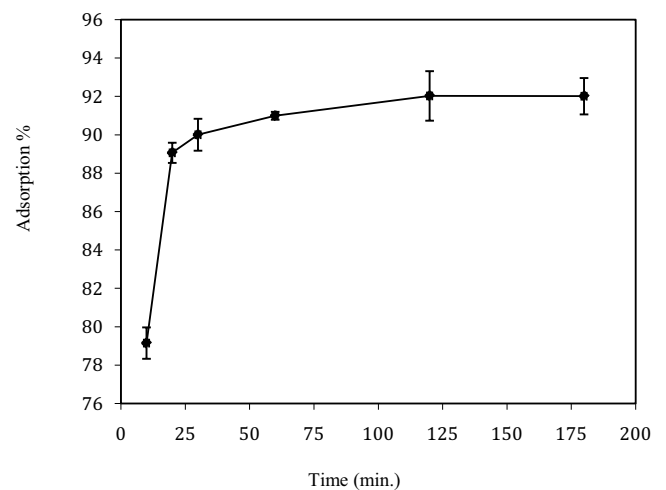


Fig. 6. Time dependency in cesium removal procedure.

Table 1  
Effect of the added solution on the distribution coefficient of cesium ions on PANI-MMT

Added cation	$K_d$ (mL/g)
None	228.74
$Na^+$	63.88
$K^+$	59.24
$Ca^{2+}$	76.34
$Mg^{2+}$	75.90

### 3.2.5. Adsorption isotherms

Langmuir and Freundlich models were used for identification of the isotherm data. Both linear isotherm equations are expressed as follows:

$$\text{Langmuir: } \frac{C}{q_e} = \frac{C}{q_m b} + \frac{C}{q_m} \quad (1)$$

$$\text{Freundlich: } \ln q_e = \ln K_F + \frac{1}{n_F} \ln C_e \quad (2)$$

where  $C_e$  is the equilibrium concentration of  $\text{Cs}^+$  ion,  $q_e$  is the adsorption amount of  $\text{Cs}^+$  per unit weight of PANI/MMT at equilibrium,  $q_m$  is the maximum monolayer sorption capacity (mg/g),  $b$  is the Langmuir constant related to the affinity of binding sites,  $K_F$  and  $n_F$  are Freundlich constants related to adsorption capacity and adsorption intensity.  $Q^0$  (mg/g) is the maximum adsorption at monolayer.

Figs. 8 and 9, respectively, show the Langmuir and Freundlich isotherm plots fitted for the cesium adsorption on the adsorbent. The parameters of Langmuir and Freundlich isotherms that can be calculated from the slopes and intercepts of these plots are listed in Table 2.

It can be inferred from this table that the higher correlation coefficients for the Langmuir model show that the adsorption of cesium ions into the PANI/MMT correlates well with the Langmuir equation in comparison with the Freundlich model.

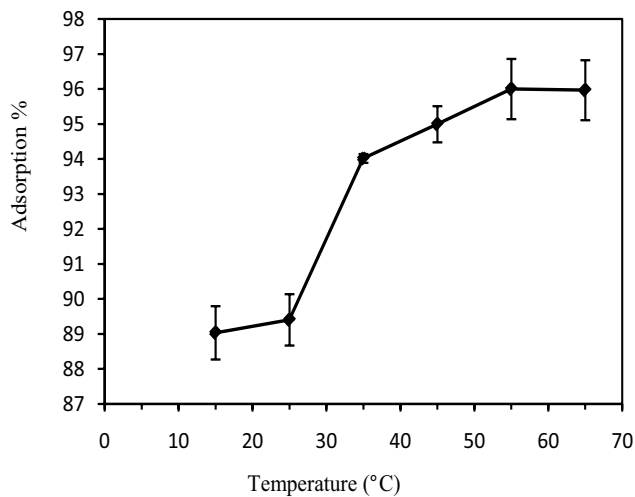


Fig. 7. Temperature effect on Cs removal.

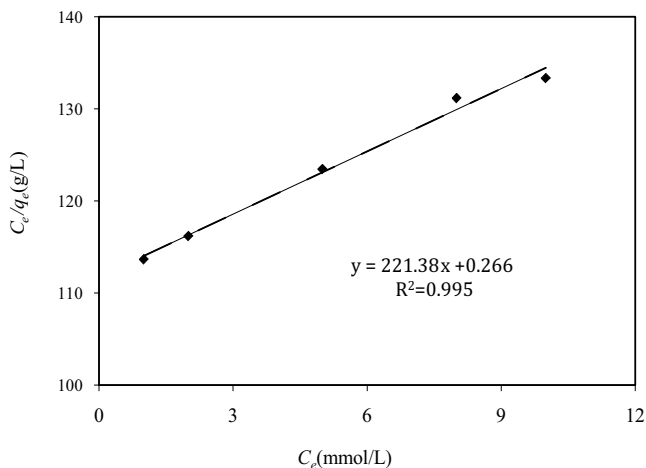


Fig. 8. Langmuir adsorption isotherm of Cs on PANI/MMT.

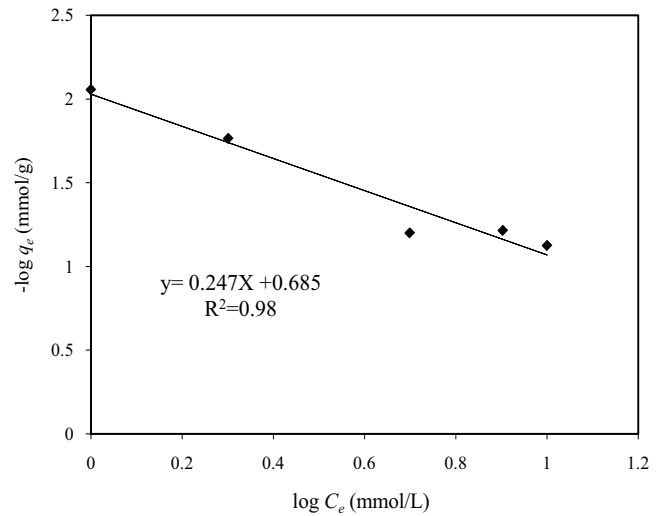


Fig. 9. Freundlich adsorption isotherm of Cs on PANI/MMT.

Table 2  
Langmuir and Freundlich constants

Langmuir constants			Freundlich constants		
$Q^0$ (mg/g)	$b$ (L/mg)	$R^2$	$K_f$ (mg/g)	$N_f$	$R^2$
0.0045	90.09	0.995	1.15	0.07	0.98

### 3.2.6. Thermodynamic investigation

Thermodynamic parameters for the adsorption such as enthalpy change, entropy and free energy change were calculated by the following equations,

$$\ln K_d = \frac{\Delta S^\circ}{R} - \frac{\Delta H^\circ}{RT} \quad (3)$$

$$\Delta G^\circ = \Delta H^\circ - T\Delta S^\circ \quad (4)$$

where  $\Delta H^\circ$  is standard enthalpy,  $\Delta S^\circ$  is standard entropy,  $\Delta G^\circ$  is standard Gibbs free energy,  $R$  is the ideal gas constant in  $\text{J mol}^{-1} \text{K}^{-1}$ ,  $T$  is the absolute temperature in Kelvin and  $K_d$  is the thermodynamic equilibrium constant in liter per mole. By calculating the slope and intercept of the  $\ln K_d$  vs.  $1/T$  plot (Fig. 10), the values of  $\Delta H^\circ$  and  $\Delta S^\circ$  were obtained.

The values of  $\Delta H^\circ$ ,  $\Delta S^\circ$  and  $\Delta G^\circ$  parameters are summarized in Table 3. The positive value of  $\Delta H^\circ$  and the decrease in the value of  $\Delta G^\circ$  with the increase in temperature indicate that the ion-exchange process is an endothermic and more favorable reaction. The positive value of  $\Delta S^\circ$  makes  $\Delta G$  negative, which indicates the spontaneity of the sorption process.

### 3.2.7. Comparison of different adsorption efficiencies

Table 4 summarizes adsorption efficiencies determined from previous studies. As can be deduced from the table, the efficiency of cesium removal by synthesized adsorbent in this study was higher than the values obtained by Yang et al. [7], Saberi et al. [11] and Nilchi et al. [13] which removed

Table 3  
Thermodynamics parameters of PANI/MMT

Temperature (K)	$-\Delta G^\circ$ (kJ mol <sup>-1</sup> )	$\Delta H^\circ$ (kJ mol <sup>-1</sup> )	$\Delta S^\circ$ (kJ kmol <sup>-1</sup> )
283	-13,291.3 8		
293	-13,761.06		
303	-14,230.70	0.56	46.968
333	-15,639.78		
393	-18,454.72		

Table 4  
Comparison of removal efficiency from aqueous solutions cited in the literature with the present study

Adsorbent	Temperature (°C)	Contact time (h)	Efficiency (percentage)	Reference
PANI-MMT	55	120	96	This study
Bentonite and carbon nanotube	55	900	80	Yang et al. [7]
Sodium titanosilicate-PAN	55	150	76	Saberi et al. [11]
Cerium molybdate-PAN	55	25	49	Nilchi et al. [13]

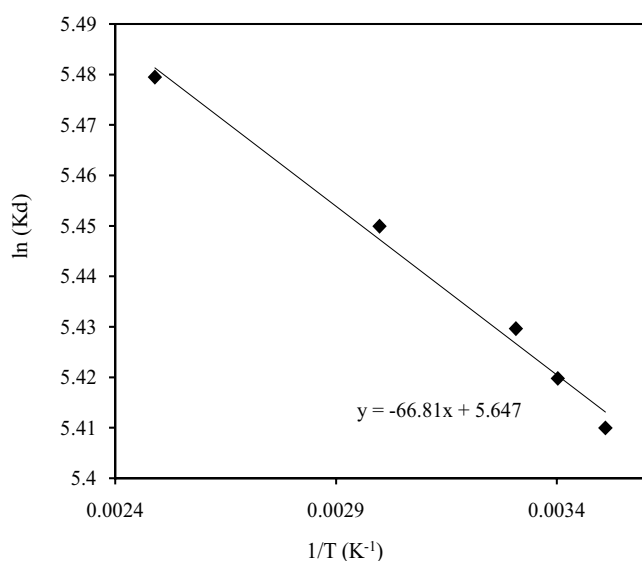


Fig. 10. Effect of solution temperature on the distribution coefficient of Cs ion on PANI/MMT.

cesium from aqueous solution with efficiency of 80%, 76% and 49%, respectively.

#### 4. Conclusion

In this study, polyaniline montmorillonite (PANI/MMT) composite ion exchanger was successfully synthesized and characterized by various physicochemical techniques. The synthesized composite adsorbent had a crystalline structure. The effects of some parameters, including solution pH, contact time and solution temperature were studied on the cesium adsorption by the prepared adsorbent, comprehensively. It was observed that the adsorption efficiency of PANI/MMT is strongly affected by the initial solution pH

and the increase of pH, contact time and temperature have positive effects on the adsorption process.

In addition, it is proved that the optimum time and temperature for interaction between cesium and PANI/MMT sorbent are 120 min and 55°C, respectively. PANI/MMT sorbent showed high adsorption of cesium removal from aqueous solution (96%) with initial cesium concentration equal to 50 mg/L. On the other hand, the distribution coefficient of cesium ions decreased by adding the interfering cations to the aqueous solution.

The obtained equilibrium data indicated that the cesium sorption on the adsorbent better correlates with the Langmuir isotherm equation than the Freundlich model. The apparent values of  $\Delta H^\circ$ ,  $\Delta G^\circ$  and  $\Delta S^\circ$  proved that the cesium adsorption on synthesized ion exchange composite is an endothermic and spontaneous process.

Based on these results, it can be concluded that PANI/MMT composite would be an effective sorbent for the removal of cesium from aqueous solutions.

#### References

- [1] P.K. Goel, Water Pollution: Causes, Effects and Control, New Age International, 2006.
- [2] A.M. El-Kamash, A.A. Zaki, M. Abed El Geleel, Modeling batch kinetics and thermodynamics of zinc and cadmium ions removal from waste solutions using synthetic zeolite A, *J. Hazard. Mater.*, 127 (2005) 211–220.
- [3] S.N. Groudev, S.G. Bratcova, K. Komnitsas, Treatment of waters polluted with radioactive elements and heavy metals by means of a laboratory passive system, *Miner. Eng.*, 12 (1999) 261–270.
- [4] E.D. Goldberg, *The Health of the Oceans*, ERIC, 1976, pp. 172.
- [5] S. Pande, H. Swaruparani, M.D. Bedre, R. Bhat, R. Deshpande, A. Venkataraman, Synthesis, characterization and studies of PANI-MMT nanocomposites, *Nanosci. Nanotechnol.*, 2 (2012) 90–98.
- [6] H. Van Hoang, R. Holze, Electrochemical synthesis of polyaniline/montmorillonite nanocomposites and their characterization, *Chem. Mater.*, 18 (2006) 1976–1980.

- [7] D. Yang, S. Sarina, H. Zhu, H. Liu, Z. Zheng, M. Xie, S.V. Smith, S. Komarneni, Capture of radioactive cesium and iodide ions from water by using titanate nanofibers and nanotubes, *Angewandte Chemie*, 123 (2011) 10782–10786.
- [8] Y. Park, Y.C. Lee, W.S. Shin, S.J. Choi, Removal of cobalt, strontium and cesium from radioactive laundry wastewater by ammonium molybdophosphate–polyacrylonitrile (AMP–PAN), *Chem. Eng. J.*, 162 (2010) 685–695.
- [9] H.D. Liu, F.Z. Li, X. Zhao, G.C. Yun, Preparing high-loaded potassium cobalt hexacyanoferrate/silica composite for radioactive wastewater treatment, *Nucl. Technol.*, 165 (2009) 200–208.
- [10] V.V. Milyutin, O.A. Kononenko, S.V. Mikheev, V.M. Gelis, Sorption of cesium on finely dispersed composite ferrocyanide sorbents, *Radiochemistry*, 52 (2010) 281–283.
- [11] R. Saberi, A. Nilchi, S. Rasouli Garmarodi, R. Zarghami, Adsorption characteristic of <sup>137</sup>Cs from aqueous solution using PAN-based sodium titanate composite, *J. Radioanal. Nucl. Chem.*, 284 (2010) 461–469.
- [12] A. Nilchi, R. Saberi, M. Moradi, H. Azizpour, R. Zarghami, Adsorption of cesium on copper hexacyanoferrate–PAN composite ion exchanger from aqueous solution, *Chem. Eng. J.*, 172 (2011) 572–580.
- [13] A. Nilchi, R. Saberi, H. Azizpour, M. Moradi, R. Zarghami, M. Naushad, Adsorption of caesium from aqueous solution using cerium molybdate–pan composite, *Chem. Ecol.*, 28 (2012) 169–185.
- [14] A. Nilchi, H. Atashi, A.H. Javid, R. Saberi, Preparations of PAN-based adsorbents for separation of cesium and cobalt from radioactive wastes, *Appl. Radiat. Isotopes*, 65 (2007) 482–487.
- [15] A. Nilchi, R. Saberi, M. Moradi, H. Azizpour, R. Zarghami, Evaluation of AMP–PAN composite for adsorption of Cs<sup>+</sup> ions from aqueous solution using batch and fixed bed operations, *J. Radioanal. Nucl. Chem.*, 292 (2012) 609–617.
- [16] A. Nilchi, R. Saberi, S.R. Garmarodi, A. Bagheri, Evaluation of PAN-based manganese dioxide composite for the sorptive removal of cesium-137 from aqueous solutions, *Appl. Radiat. Isotopes*, 70 (2012) 369–374.
- [17] N. Ding, M.G. Kanatzidis, Selective incarceration of caesium ions by Venus flytrap action of a flexible framework sulfide, *Nature Chem.*, 2 (2010) 187.
- [18] R.O. Rahman, H.A. Ibrahim, Y.T. Hung, Liquid radioactive wastes treatment: a review, *Water*, 3 (2011) 551–565.
- [19] Z. Ahmad, The Removal of uranium from aqueous solution, *J. Nucl. Related Technol.*, 9 (2012) 109–120.
- [20] X. Ren, C. Chen, M. Nagatsu, X. Wang, Carbon nanotubes as adsorbents in environmental pollution management: a review, *Chem. Eng. J.*, 170 (2011) 395–410.
- [21] V.K. Upadhyayula, S. Deng, M.C. Mitchell, G.B. Smith, Application of carbon nanotube technology for removal of contaminants in drinking water: a review, *Sci. Total Environ.*, 408 (2009) 1–13.
- [22] S. Agnihotri, J.P. Mota, M. Rostam-Abadi, M.J. Rood, Structural characterization of single-walled carbon nanotube bundles by experiment and molecular simulation, *Langmuir*, 21 (2005) 896–904.
- [23] C. Chen, J. Hu, D. Xu, X. Tan, Y. Meng, X. Wang, Surface complexation modeling of Sr (II) and Eu (III) adsorption onto oxidized multiwall carbon nanotubes, *J. Colloid Interface Sci.*, 323 (2008) 33–41.
- [24] C.L. Chen, X.K. Wang, M. Nagatsu, Europium adsorption on multiwall carbon nanotube/iron oxide magnetic composite in the presence of polyacrylic acid, *Environ. Sci. Technol.*, 43 (2009) 2362–2367.
- [25] M.A. Tofighy, Y. Shirazi, T. Mohammadi, A. Pak, Salty water desalination using carbon nanotubes membrane, *Chem. Eng. J.*, 168 (2011) 1064–1072.
- [26] J. Vejsada, E. Jelínek, Z. Řanda, D. Hradil, R. Přikryl, Sorption of cesium on smectite-rich clays from the Bohemian Massif (Czech Republic) and their mixtures with sand, *Appl. Radiat. Isotopes*, 62 (2005) 91–96.
- [27] Y. Park, W.S. Shin, G.S. Reddy, S.J. Shin, S.J. Choi, Use of nano crystalline silicotitanate for the removal of Cs, Co and Sr from low-level liquid radioactive waste, *J. Nanoelect. Optoelectr.*, 5 (2010) 238–242.
- [28] M. Galamboš, J. Kufčáková, O.G. Rosskopfová, P. Rajec, Adsorption of cesium and strontium on natrified bentonites, *J. Radioanal. Nucl. Chem.*, 283 (2009) 803–813.
- [29] A. Ararem, O. Bouras, F. Arbaoui, Adsorption of caesium from aqueous solution on binary mixture of iron pillared layered montmorillonite and goethite, *Chem. Eng. J.*, 172 (2011) 230–236.
- [30] D. Fan, X. Zhu, M. Xu, J. Yan, Adsorption properties of chromium (VI) by chitosan coated montmorillonite, *J. Biol. Sci.*, 6 (2006) 941–945.
- [31] S.A. Khan, Sorption of the long-lived radionuclides cesium-134, strontium-85 and cobalt-60 on bentonite, *J. Radioanal. Nucl. Chem.*, 258 (2003) 3–6.
- [32] E.T. Kang, K.G. Neoh, K.L. Tan, Polyaniline: a polymer with many interesting intrinsic redox states, *Progr. Polym. Sci.*, 23 (1998) 277–324.
- [33] S. Yoshimoto, F. Ohashi, Y. Ohnishi, T. Nonami, Synthesis of polyaniline–montmorillonite nanocomposites by the mechanochemical intercalation method, *Synth. Metals*, 145 (2004) 265–270.
- [34] J. Wu, B. Li, J. Liao, Y. Feng, D. Zhang, J. Zhao, N. Liu, Behavior and analysis of cesium adsorption on montmorillonite mineral, *J. Environ. Radioact.*, 100 (2009) 914–920.